ISSN 1392–1320 MATERIALS SCIENCE (MEDŽIAGOTYRA). Vol. 26, No. 2. 2020

Hydriding and Dehydriding Features of a Titanium-Added Magnesium Hydride Composite

Eunho CHOI [1], Myoung Youp SONG [2] *

[1] *Department of Materials Engineering, Graduate School, Jeonbuk National University, 567 Baekje-daero Deokjin-gu Jeonju, 54896, Republic of Korea*
[2] *Division of Advanced Materials Engineering, Hydrogen & Fuel Cell Research Center, Engineering Research Institute, Jeonbuk National University, 567 Baekje-daero Deokjin-gu Jeonju, 54896, Republic of Korea*

crossref http://dx.doi.org/10.5755/j01.ms.26.2.22299

Received 14 December 2018; accepted 01 February 2019

Magnesium has excellent hydrogen-storage properties except low hydriding and dehydriding rates. In the present work, titanium (Ti) was chosen as an additive to increase the hydriding rate of Mg and the dehydriding rate of MgH_2. 15 wt.% Ti was added to MgH_2 by milling in hydrogen (reactive mechanical grinding). The hydriding and dehydriding features of the Ti-added MgH_2 composite (named 85 MgH_2 + 15 Ti) were investigated. At the first cycle (n = 1), 85 MgH_2 + 15 Ti absorbed 2.96 wt.% H for 2.5 min and 5.51 wt.% H for 60 min at 593 K in 12 bar H_2, having an effective hydrogen-storage capacity of 5.51 wt.%. β-MgH_2, γ-MgH_2, $TiH_{1.924}$, MgO, and $MgTi_2O_4$ were formed during reactive mechanical grinding. Reactive mechanical grinding of MgH_2 with Ti is believed to create imperfections, produce cracks and clean surfaces, and decrease particle sizes. The phases formed during reactive mechanical grinding and their pulverization during reactive mechanical grinding are believed to make these effects stronger.

Keywords: hydrogen-storage materials, milling in hydrogen, hydriding and dehydriding rates, hydrogen-storage capacity titanium-added magnesium hydride.

1. INTRODUCTION

Magnesium (Mg) has excellent hydrogen-storage features, but it has low hydriding and dehydriding rates. To increase the reaction rates of Mg with hydrogen, many researches were carried out by adding added to Mg or MgH_2 transition metals [1 – 4], rare-earth metals [5], graphite [6, 7], or intermetallic compounds [8 – 10] have been added to Mg or MgH_2.

Rizo-Acosta et al. [11] added different amounts of Ti to magnesium to form MgH_2-TiH_2 nanocomposites by reactive ball milling under hydrogen gas. On increasing Ti amount, hydriding and dehydriding kinetics were enhanced leading to a higher reversibility for hydrogen storage with the MgH_2 phase. The highest reversible capacity (4.9 wt.% H) was obtained for the lowest TiH_2 content (y = 0.025). Sohn et al. [12] reported that the MgH_2 doped with TiH_2 by high-energy milling displayed substantially reduced apparent activation energy and significantly faster kinetics, compared with similarly milled MgH_2 without TiH_2 doping. Daryani et al. [13] investigated the co-effects of Ti-based catalysts (TiH_2 and TiO_2 particles) on hydrogen desorption kinetics of nanostructured magnesium hydride. The samples were prepared by high-energy ball milling. Evaluation of the absorption/desorption properties revealed that the addition of the Ti-based catalysts significantly improved the hydrogen storage performance of MgH_2. A decrease in the decomposition temperature (as high as 100 K) was attained after co-milling of MgH_2 with the Ti-based catalysts.

In the present work, titanium (Ti) was chosen as an additive to improve the hydriding and dehydriding features of MgH_2. 15 wt.% Ti was added to MgH_2 by milling in hydrogen (reactive mechanical grinding). The hydriding and dehydriding features of the Ti-added MgH_2 composite (named MgH_2-15Ti) were investigated.

2. EXPERIMENTAL DETAILS

We used MgH_2 powder (magnesium hydride, hydrogen storage grade, Sigma Aldrich.) and titanium (-3.25 mesh, 99.5 % metal basis, Alfa Aesar) as starting materials.

Reactive mechanical grinding to prepare a 85 MgH_2 + 15 Ti sample, which has a composition of 85 wt.% Mg + 15 wt.% Ti, was performed in a planetary ball mill (Planetary Mono Mill; Pulverisette 6, Fritsch). Mixtures with the desired compositions (8 g) were milled in a hermetically sealed stainless steel container with 105 hardened steel balls (total weight 360 g). All sample handling was performed in a glove box under Ar in order to prevent oxidation. The disc revolution speed was 250 rpm. The mill container with a volume of 250 mL was then filled with high purity hydrogen gas (~ 12 bar). Milling was performed for 6 h, refilling hydrogen up to ~ 12 bar every two hours [14 – 17].

The absorbed or released hydrogen quantity, as the reaction time elapses, was measured in nearly constant hydrogen pressures (in 12 bar H_2 for hydriding and in 1.0 bar H_2 for dehydriding) with the Sieverts' type hydriding and dehydrding apparatus described previously [18 – 22]. 0.5 g of the samples was used for these measurements.

* Corresponding author. Tel.: +82-63-270-2379; fax: +82-63-270-2386.
E-mail address: *songmy@jbnu.ac.kr* (M.Y. Song)

Samples after reactive mechanical grinding and after hydriding-dehydrding cycling were analysed by X-ray diffraction (XRD) with Cu Kα radiation, using a Rigaku D/MAX 2500 powder diffractometer. The microstructures of the powders were observed using a JSM-5900 scanning electron microscope (SEM) operated at 20 kV.

3. RESULTS AND DISCUSSION

Fig. 1 shows the variation in H_a versus t curve with cycle number, n, at 573 K in 12 bar H_2 for 85 M g H_2 + 15 Ti. At n = 1, the initial hydriding rate is quite high and the quantity of hydrogen absorbed for 60 min, H_a (60 min), is quite large. At n = 1, the hydriding rate decreases gradually as the reaction time elapses and is very low after 20 min. As n increases from one to four, the initial hydriding rate and H_a (60 min) decrease in general. The general decreases in the initial hydriding rate and H_a (60 min) with the increase in the cycle number are believed to be due to coalescence of particles since the sample was maintained at the relatively high temperature 573 K during hydriding-dehydriding cycling. At n = 1, 85 MgH_2 + 15 Ti absorbs 1.58 wt.% H for 2.5 min, 2.67 wt.% H for 10 min, and 3.44 wt.% H for 60 min. At n = 4, 85 MgH_2 + 15 Ti absorbs 1.40 wt.% H for 2.5 min, 2.44 wt.% H for 10 min, and 3.21 wt.% H for 60 min. Table 1 shows the variation of H_a with t at 573 K in 12 bar H_2 at n = 1 ~ 4 for 85 MgH_2 + 15 Ti.

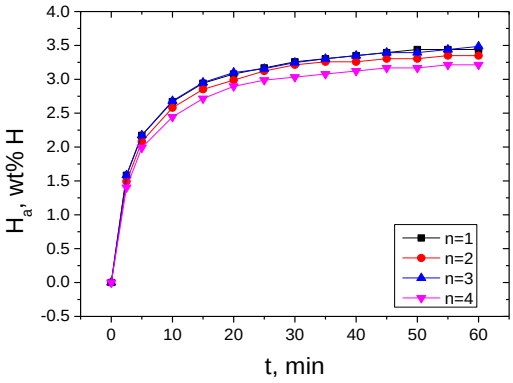

Fig. 1. Variation in H_a versus t curve with cycle number, n, at 573 K in 12 bar H_2 for 85 MgH_2 + 15 Ti

Table 1. Variation of H_a (wt.% H) with t (min) at 573 K in 12 bar H_2 at n = 1 ~ 4 for 85 MgH_2 + 15 Ti

	2.5 min	5 min	10 min	30 min	60 min
n=1	1.58	2.17	2.67	3.26	3.44
n=2	1.49	20.08	2.58	3.21	3.35
n=3	1.58	2.17	2.68	3.25	3.48
n=4	1.40	1.99	2.44	3.02	3.21

We define the quantity of hydrogen absorbed for 60 min as the effective hydrogen storage capacity. 85 MgH_2 + 15 Ti has an effective hydrogen-storage capacity of 3.44 wt.% at 573 K in 12 bar H_2 at n = 1. The variation in H_d versus t curve with cycle number, n, at 573 K in 1.0 bar H_2 for 85 MgH_2 + 15 Ti is shown in Fig. 2. At n = 1, the initial dehydriding rate is slightly high and the quantity of hydrogen released for 60 min, H_d (60 min), is small.

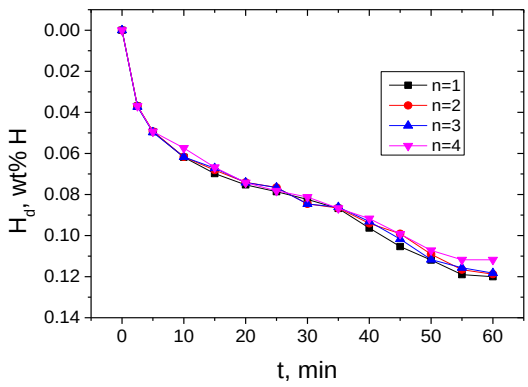

Fig. 2. Variation in H_d versus t curve with cycle number, n, at 573 K in 1.0 bar H_2 for 85 MgH_2 + 15 Ti

The slightly high initial dehydriding rate is believed to be due to the slightly large quantities of hydrogen desorbed from the surfaces of the particles and released from the Mg-H solid solution. As n increases from one to four, the initial dehydriding rates are the same and H_d (60 min) decreases. The general decrease in the H_d (60 min) with the increase in the cycle number is believed to be due to coalescence of particles since the sample was maintained at the relatively high temperature 573 K during hydriding-dehydriding cycling. At n = 1, 85 MgH_2 + 15 Ti releases 0.04 wt.% H for 2.5 min, 0.06 wt.% H for 10 min, and 0.12 wt.% H for 60 min. At n = 4, 85 MgH_2 + 15 Ti releases 0.0.04 wt.% H for 2.5 min, 0.06 wt.% H for 10 min, and 0.11 wt.% H for 60 min. Table 2 shows the variation of H_d with t at 573 K in 1.0 bar H_2 at n = 1 ~ 4 for 85 MgH_2 + 15 Ti.

Table 2. Variation of H_d (wt.% H) with t (min) at 573 K in 1.0 bar H_2 at n = 1 ~ 4 for 85 MgH_2 + 15 Ti

	2.5 min	5 min	10 min	30 min	60 min
n=1	0.04	0.05	0.06	0.08	0.12
n=2	0.04	0.05	0.06	0.08	0.12
n=3	0.04	0.05	0.06	0.08	0.12
n=4	0.04	0.05	0.06	0.08	0.11

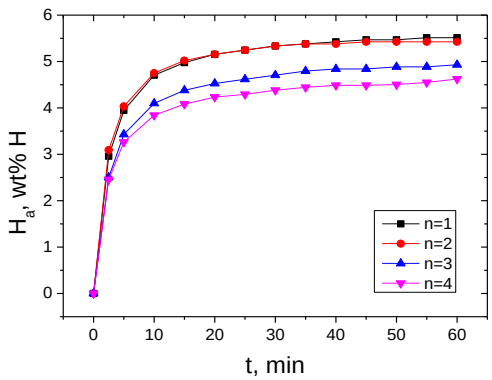

Fig. 3. Variation in H_a versus t curve with cycle number at 593 K in 12 bar H_2 for 85 MgH_2 + 15 Ti

Fig. 3 shows the variation in H_a versus t curve with cycle number, n, at 593 K in 12 bar H_2 for 85 MgH_2 + 15 Ti. At n = 1, the initial hydriding rate is quite high and the H_a (60 min) is quite large. The hydriding rate decreases gradually as the reaction time elapses and is

very low after 20 min. As n increases from one to four, the initial hydriding rate decreases in general and the H_a (60 min) decreases. At n = 1, 85 MgH_2 + 15 Ti absorbs 2.96 wt.% H for 2.5 min, 4.70 wt.% H for 10 min, and 5.51 wt.% H for 60 min. At n = 4, 85 MgH_2 + 15 Ti absorbs 2.46 wt.% H for 2.5 min, 3.84 wt.% H for 10 min, and 4.62 wt.% H for 60 min. Table 3 shows the variation of H_a with t at 593 K in 12 bar H_2 at n = 1 ~ 4 for 85 MgH_2 + 15 Ti. The initial hydriding rate is higher and the H_a (60 min) is larger at 593 K than those at 573 K.

Table 3. Variation of H_a (wt.% H) with t (min) at 593 K in 12 bar H_2 at n = 1 ~ 4 for 85 MgH_2 + 15 Ti

	2.5 min	5 min	10 min	30 min	60 min
n=1	2.96	3.94	4.70	5.33	5.51
n=2	3.09	4.03	4.75	5.33	5.42
n=3	2.50	3.42	4.09	4.70	4.93
n=4	2.46	3.26	3.84	4.38	4.62

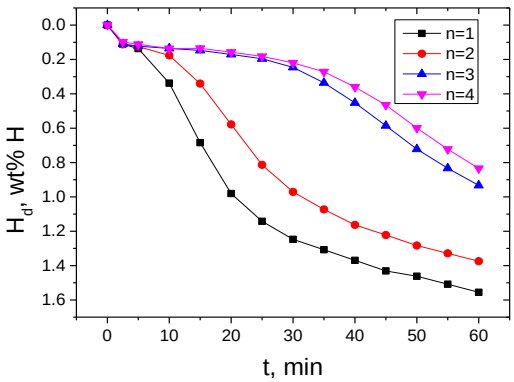

Fig. 4. Variation in H_d versus t curve with cycle number at 593 K in 1 bar H_2 for 85 MgH_2 + 15 Ti

The variation in H_d versus t curve with cycle number, n, at 593 K in 1.0 bar H_2 for 85 MgH_2 + 15 Ti is shown in Fig. 4. At n = 1, the initial dehydriding rate is slightly high and the H_d (60 min) is larger, compared with those at 573 K. As n increases from one to four, the initial dehydriding rate decreases slightly and H_d (60 min) decrease. At 2.5 min, the dehydriding rates are low. The dehydriding rates increase gradually after 2.5 min and are quite high at 10 min at n = 1, 15 min at n = 2, and 45 min at n = 3 and n = 4. At n = 1, 85 MgH_2 + 15 Ti releases 0.11 wt.% H for 2.5 min, 0.34 wt.% H for 10 min, and 1.56 wt.% H for 60 min. At n = 4, 85 MgH_2 + 15 Ti releases 0.09 wt.% H for 2.5 min, 0.14 wt.% H for 10 min, and 0.83 wt.% H for 60 min. Table 4 shows the variation of H_d with t at 593 K in 1.0 bar H_2 at n = 1 ~ 4 for 85 MgH_2 + 15 Ti.

Table 4. Variation of H_d (wt.% H) with t (min) at 593 K in 1.0 bar H_2 at n = 1 ~ 4 for 85 MgH_2 + 15 Ti

	2.5 min	5 min	10 min	30 min	60 min
n=1	0.11	0.14	0.34	1.25	1.56
n=2	0.11	0.13	0.18	0.97	1.37
n=3	0.11	0.12	0.14	0.25	0.93
n=4	0.09	0.11	0.14	0.22	0.83

The initial dehydriding rate is higher and H_d (60 min) is larger at 593 K than those at 573 K, probably because the temperature is higher and the difference between the equilibrium plateau pressure of Mg-H system and the applied hydrogen pressure (1.0 bar H_2) at 593 K is larger than that at 573 K.

Fig. 1 – Fig. 4 show that the activation of 85 MgH_2 + 15 Ti is not necessary. However, the cycling performance of 85 MgH_2 + 15 Ti is not good. Studies to improve the cycling performance of 85 MgH_2 + 15 Ti are going to be performed in our future work.

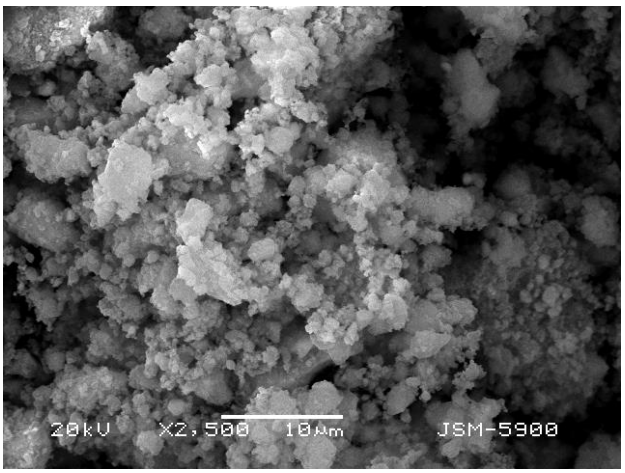

Fig. 5. A SEM micrograph of 85 MgH_2 + 15 Ti after reactive mechanical grinding

Fig. 5 shows a SEM micrograph of 85 MgH_2 + 15 Ti after reactive mechanical grinding. Particle size is not homogeneous; some particles are fine and some particles are large. These particles form agglomerates.

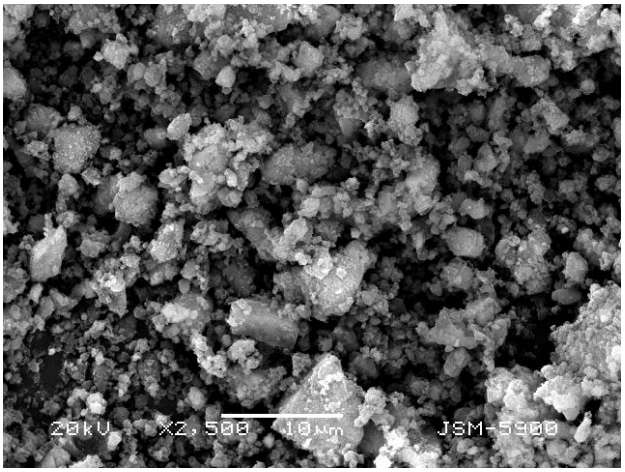

Fig. 6. A SEM micrograph of 85 MgH_2 + 15 Ti dehydrided in 1.0 bar H_2 at n = 4

A SEM micrograph of 85 MgH_2 + 15 Ti dehydrided in 1.0 bar H_2 at n = 4 is shown in Fig. 6. Particle size is not homogeneous, either; some particles are fine and some particles are large. These particles form agglomerates. Particles and agglomerates are smaller than those of the sample after reactive mechanical grinding, probably due to pulverization of the particles owing to expansion (by hydriding reaction) and contraction (by dehydriding reaction) with hydriding-dehydriding cycling [23 – 28].

Fig. 7 shows the XRD pattern of 85 MgH_2 + 15 Ti after reactive mechanical grinding. The 85 MgH_2 + 15 Ti after reactive mechanical grinding contains a large amount

of β-MgH_2 and small amounts of Mg, γ-MgH_2, $TiH_{1.924}$, MgO, and $MgTi_2O_4$. This shows that $TiH_{1.924}$ is formed by the reaction of Ti with hydrogen during milling in hydrogen. Huot et al. [29] reported that the synthesis of magnesium hydride by reactive ball milling leads to the formation of a metastable orthorhombic γ-MgH_2 phase along with tetragonal β-MgH_2.

The XRD pattern of 85 MgH_2 + 15 Ti dehydrided in 1.0 bar H_2 at n = 4 is shown in Fig. 8. The 85 MgH_2 + 15 Ti dehydrided in 1.0 bar H_2 at the 4th hydriding-dehydriding cycle contains large amounts of β-MgH_2 and Mg and very small amounts of MgO, $MgTi_2O_4$, $TiH_{1.924}$, and $Mg(OH)_2$. $TiH_{1.924}$ remains undecomposed, but γ-MgH_2 disappeared, after the sample was dehydrided in 1.0 bar H_2 at n = 4. $MgTi_2O_4$ and MgO are believed to be formed by the reaction with oxygen adsorbed on the particle surfaces during treating the samples to obtain the XRD pattern. $Mg(OH)_2$ is believed to be formed by the reaction with water vapor adsorbed on the particle surfaces during treating the samples to obtain the XRD pattern.

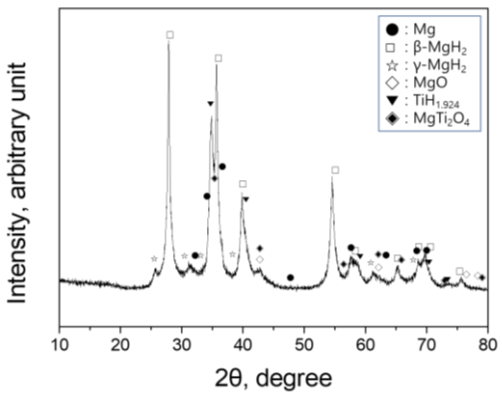

Fig. 7. XRD pattern of 85 MgH_2 + 15 Ti after reactive mechanical grinding

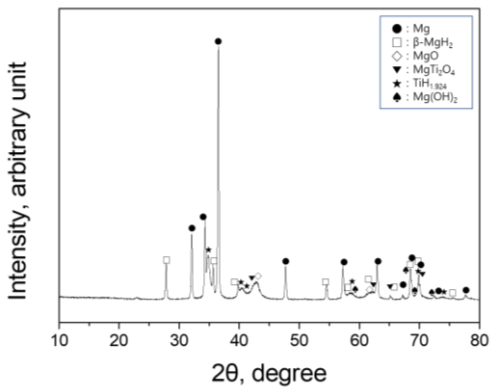

Fig. 8. XRD pattern of 85 MgH_2 + 15 Ti dehydrided in 1.0 bar H_2 at n = 4

Reactive mechanical grinding of MgH_2 with Ti is believed to create defects (leading to facilitation of nucleation), produce cracks and clean surfaces (leading to increase in reactivity), and decrease particle sizes (leading to diminution of diffusion distances or increasing the flux of the diffusing hydrogen atoms) [30 – 36]. Decrease in the particle sizes leads to the increase in the specific surface area of the sample. The β-MgH_2, γ-MgH_2, $TiH_{1.924}$, MgO, and $MgTi_2O_4$ formed during reactive mechanical grinding and their pulverization during reactive mechanical grinding are believed to make these effects stronger. The hydriding-dehydriding cycling is also believed to create defects, produce cracks and clean surfaces, and decrease particle sizes due to expansion (by hydriding reaction) and contraction (by dehydriding reaction) of Mg [37 – 42]. These effects of reactive mechanical grinding and hydriding-dehydriding cycling are believed to have improved the hydriding and dehydriding features of MgH_2.

4. CONCLUSIONS

Titanium was chosen as an additive to improve the hydriding and dehydriding features of MgH_2. 15 wt.% Ti was added to MgH_2 by reactive mechanical grinding. At the first cycle, 85 MgH_2 + 15 Ti absorbed 2.96 wt.% H for 2.5 min and 5.51 wt.% H for 60 min at 593 K in 12 bar H_2, having an effective hydrogen-storage capacity of 5.51 wt.%. 85 MgH_2 + 15 Ti released 0.11 wt.% H for 2.5 min and 1.56 wt.% H for 60 min at 593 K in 1.0 bar H_2 at n = 1. Reactive mechanical grinding of MgH_2 with Ti is believed to create defects, produce cracks and clean surfaces, and decrease particle sizes. The β-MgH_2, γ-MgH_2, $TiH_{1.924}$, MgO, and $MgTi_2O_4$ formed during reactive mechanical grinding and their pulverization during reactive mechanical grinding are believed to make these effects stronger. The hydriding-dehydriding cycling is also believed to bring about the effects similar to those of reactive mechanical grinding.

Acknowledgements

This research was supported by Basic Science Research Program through the National Research Foundation of Korea (NRF) funded by the Ministry of Education (grant number NRF-2017R1D1A1B03030515).

REFERENCES

1. **Krozer, A., Kasemo, B.** Equilibrium Hydrogen Uptake and Associated Kinetics for the Mg-H_2 System at Low Pressures *Journal of Physics: Condensed Matter* 1 (8) 1989: pp. 1533 – 1538. https://doi.org/10.1088/0953-8984/1/8/017
2. **Karty, A., Genossar, J.G., Rudman, P.S.** Hydriding and Dehydriding Kinetics of Mg in a Mg/Mg_2Cu Eutectic Alloy: Pressure Sweep Method *Journal of Applied Physics* 50 (11) 1979: pp. 7200 – 7209. https://doi.org/10.1063/1.325832
3. **Bobet, J.L. Akiba, E., Nakamura, Y., Darriet, B.** Study of Mg-M (M=Co, Ni and Fe) Mixture Elaborated by Reactive Mechanical Alloying-Hydrogen Sorption Properties *International Journal of Hydrogen Energy* 25 (10) 2000: pp. 987 – 996. https://doi.org/10.1016/S0360-3199(00)00082-3
4. **Reilly, J.J., Wiswall, R.H.** Reaction of Hydrogen with Alloys of Magnesium and Copper *Inorganic Chemistry* 7 (11) 1968: pp. 2254 – 2256. https://doi.org/10.1021/ic50058a020
5. **Tran, N.E., Imam, M.A., Feng, C.R.** Evaluation of Hydrogen Storage Characteristics of Magnesium–Misch Metal Alloys *Journal of Alloys Compounds* 359 (1 – 2) 2003: pp. 225 – 229. https://doi.org/10.1016/S0925-8388(03)00176-2

6. **Huot, J., Tremblay, M.L., Schulz, R.** Synthesis of Nanocrystalline Hydrogen Storage Materials *Journal of Alloys Compounds* 356 – 357 2003: pp. 603 – 607. https://doi.org/10.1016/S0925-8388(03)00120-8

7. **Popilevsky, L., Skripnyuk, V.M., Beregovsky, M., Senzen, M., Amouyal, Y., Rabkin, E.** Hydrogen Storage and Thermal Transport Properties of Pelletized Porous Mg-2 wt.% Multiwall Carbon Nanotubes and Mg-2 wt.% Graphite Composites *International Journal of Hydrogen Energy* 41 (32) 2016: pp. 14461 – 14474. https://doi.org/10.1016/j.ijhydene.2016.03.014

8. **Guoxian, L., Erde, W., Shoushi, F.** Hydrogen Absorption and Desorption Characteristics of Mechanically Milled Mg-35 wt.% $FeTi_{1.2}$ Powders *Journal of Alloys Compounds* 223 (1) 1995: pp. 111 – 114. https://doi.org/10.1016/0925-8388(94)01465-5

9. **Liang, G., Boily, S., Huot, J., Neste, A.V., Schulz, R.** Hydrogen Absorption Properties of a Mechanically Milled Mg–50 wt.% $LaNi_5$ Composite *Journal of Alloys Compounds* 268 (1 – 2) 1998: pp. 302 – 307. https://doi.org/10.1016/S0925-8388(97)00607-5

10. **Khrussanova, M., Bobet, J.L., Terzieva, M., Chevalier, B., Radev, D., Peshev, P., Darriet, B.** Hydrogen Storage Characteristics of Magnesium Mechanically Alloyed with YNi_5−xAlx (x = 0, 1 and 3) Intermetallics *Journal of Alloys Compounds* 307 (1 – 2) 2000: pp. 283 – 289. https://doi.org/10.1016/S0925-8388(00)00842-2

11. **Rizo-Acosta, P., Cuevas, F., Latroche, M.** Optimization of TiH_2 Content for Fast and Efficient Hydrogen Cycling of MgH_2-TiH_2 Nanocomposites *International Journal of Hydrogen Energy* 43 2018: pp. 16774 – 16781. https://doi.org/10.1016/j.ijhydene.2018.04.169

12. **Sohn, H.Y., Emami, S.** Kinetics of Dehydrogenation of the Mg-Ti-H Hydrogen Storage System *International Journal of Hydrogen Energy* 36 2011: pp. 8344 – 8350. https://doi.org/10.1016/j.ijhydene.2011.03.167

13. **Daryani, M., Simchi, A., Sadati, M., Mdaah Hosseini, H., Targholizadeh, H., Khakbiz, M.** Effects of Ti-Based Catalysts on Hydrogen Desorption Kinetics of Nanostructured Magnesium Hydride *International Journal of Hydrogen Energy* 39 2014: pp. 21007 – 21014. https://doi.org/10.1016/j.ijhydene.2014.10.078

14. **Kwak, Y.J., Park, H.R., Song, M.Y.** Characterization of Hydrogen-Storage Properties and Physical Properties of Zinc Borohydride and Transition Metals-Added Magnesium Hydride *Materials Science (Medžiagotyra)* 23 (1) 2017: pp. 31 – 38. http://dx.doi.org/10.5755/j01.ms.23.1.14878

15. **Song, M.Y., Lee, S.H., Kwak, Y.J., Park, H.R.** Improvement in Hydrogention and Dehydrogenation Characteristics of Magnesium by Addition of Titanium (III) Chloride via Transformation-Accompanying Milling *Materials Science (Medžiagotyra)* 23 (3) 2017: pp. 227-232. http://dx.doi.org/10.5755/j01.ms.23.3.16375

16. **Park, H.R., Lee, S.H., Kwak, Y.J., Song, M.Y.** Oxide or Halide and Nickel-Added Mg by Phase Transition-Accompanying High-energy Ball Milling Processing *Journal of Ceramic Processing Research* 18 (11) 2017: pp. 824 – 830.

17. **Kwak, Y.J., Song, M.Y.** How to Analyse Metal Hydride Decomposition Temperatures Using a Sieverts' Type Hydriding-Dehydriding Apparatus and Hydrogen-Storage Characteristics for an MgH_2–Based Alloy *Materials Science (Medžiagotyra)* 24 (1) 2018: pp. 24 – 28. http://dx.doi.org/10.5755/j01.ms.24.1.17664

18. **Choi, E., Kwak, Y.J., Song, M.Y.** Development of an Mg-Based Alloy with a Hydrogen-Storage Capacity over 6 wt% by Adding Graphene *Metals and Materials International* 24 (6) 2018: pp. 1403 – 1411. https://doi.org/10.1007/s12540-018-0151-2

19. **Kwak, Y.J., Park, H.R., Song, M.Y.** Advancement in the Hydrogen Absorbing and Releasing Kinetics of MgH_2 by Mixing with Small Percentages of $Zn(BH_4)_2$ and Ni *Metals and Materials International* 22 (2) 2018: pp. 423 – 432. https://doi.org/10.1007/s12540-018-0036-4

20. **Park, H.R., Kwon, S.N., Song, M.Y.** Effects of Milling Ttime on the Hydrogen Storage Properties of Mg-Based Transition Metals-Added Alloys *Materials Science (Medžiagotyra)* 24 (2) 2018: pp. 166 – 71. http://dx.doi.org/10.5755/j01.ms.24.2.18395

21. **Kwak, Y.J., Park, H.R., Song, M.Y.** Changes in Microstructure, Phases, and Hydrogen Storage Characteristics of Metal Hydro-Borate and Nickel-Added Magnesium Hydride with Hydrogen Absorption and Release Reactions *International Journal of Hydrogen Energy* 42 (2) 2017: pp. 1018 – 1026. https://doi.org/10.1016/j.ijhydene.2016.10.097

22. **Song, M.Y., Choi, E., Kwak, Y.J.** Development of a Mg-Based Alloy with a Hydrogen-Storage Capacity of 7 wt.% by Adding a Polymer CMC via Transformation-Involving Milling *Korean Journal of Metals and Materials* 56 (5) 2018: pp. 392 – 399. https://doi.org/10.3365/KJMM.2018.56.5.392

23. **Song, M.Y., Kwak, Y.J., Lee, S.H., Park, H.R.** Increase in Hydrogen Release Rate of MgH_2 by Grinding in a Hydrogen Atmosphere with Ni Added *Journal of Nanoscience and Nanotechnology* 16 2016: pp. 10499 – 10507. https://doi.org/10.1166/jnn.2016.13184

24. **Kwak, Y.J., Lee, S.H., Park, H.R., Song, M.Y.** Hydrogen Storage Characteristics of Mg, Mg-5TaF_5, and Mg-5NbF_5 Prepared via Grinding in a Hydrogen Atmosphere *Journal of Nanoscience and Nanotechnology* 16 2016: pp. 10508 – 10514. https://doi.org/10.1166/jnn.2016.13185

25. **Kwak, Y.J., Park, H.R., Song, M.Y.** Development of a Hydrogen-Storage Alloy with a High Capacity of Approximately 6 wt.% by Adding a Transition Metal and a Halide *Journal of Nanoscience and Nanotechnology* 17 (11) 2017: pp. 8105 – 8111. https://doi.org/10.1166/jnn.2017.15083

26. **Song, M.Y., Lee, S.H., Kwak, Y.J., Park, H.R.** Cycling Performance of $NaAlH_4$ and Transition Metals-Added MgH_2 Prepared via Milling in a Hydrogen Atmosphere *Journal of Nanoscience and Nanotechnology* 17 (11) 2017: pp. 8132 – 8137. https://doi.org/10.1166/jnn.2017.15084

27. **Kwak, Y.J., Lee, S.H., Song, M.Y.** Development of an Mg-Based Alloy with High Hydriding and Dehydriding Rates and a Large Hydrogen Storage Capacity by Adding TaF_5 *Journal Nanoscience and Nanotechnology* 18 (9) 2018: pp. 6040 – 6046. https://doi.org/10.1166/jnn.2018.15607

28. **Song, M.Y., Kwak, Y.J., Lee, S.H.** Improvement of Hydrogen-Storage Characteristics of Magnesium Hydride by Grinding with Sodium Alanate and Transition Metals in Hydrogen Atmosphere *Journal Nanoscience and Nanotechnology* 18 (9) 2018: pp. 6047 – 6054. https://doi.org/10.1166/jnn.2018.15608

29. **Huot, J., Swainson, I., Schulz, R.** Changement de Phase Induit par Broyage Mecanique dans l'Hydrure de Magesium (Phase Transformation in Magnesium Hydride Induced by Ball Milling) *Annales de Chimie Science des Materiaux (Paris)* 31 (1) 2006: pp. 135 – 144.

30. **Park, H.R., Kwak, Y.J., Song, M.Y.** Increase in the Hydrogen-Sorption Rates and Hydrogen-Storage Capacity of MgH_2 by Adding a Small Proportion of $Zn(BH_4)_2$ *Korean Journal of Metals and Materials* 55 (9) 2017: pp. 656 – 662. https://doi.org/10.3365/KJMM.2017.55.9.657

31. **Hong, S.H., Kwak, Y.J., Song, M.Y.** Enhancement of the Hydrogen-Storage Characteristics of Mg by Adding Mg_2Ni and Ni to MgH_2 via High Energy Ball Milling in Hydrogen Atmosphere *Korean Journal of Metals and Materials* 56 (1) 2018: pp. 59 – 65. https://doi.org/10.3365/KJMM.2018.56.1.59

32. **Hong, S.H., Song, M.Y.** Hydrogen Absorption and Release Properties of MgH_2, Mg_2Ni, and Ni-added Mg via Reactive Mechanical Grinding *Korean Journal of Metals and Materials* 56 (2) 2018: pp. 155 – 162. https://doi.org/10.3365/KJMM.2018.56.2.141

33. **Song, M.Y., Kwak, Y.J.** Comparison of the Hydrogen Release Properties of $Zn(BH_4)_2$-Added MgH_2 Alloy and $Zn(BH_4)_2$ and Ni-added MgH_2 Alloy *Korean Journal of Metals and Materials* 56 (3) 2018: pp. 244 – 251. https://doi.org/10.3365/KJMM.2018.56.3.244

34. **Song, M.Y., Kwak, Y.J.** Hydrogen Uptake and Release Characteristics of Mg-xTaF_5-xVCl_3 (x = 1.25, 2.5, and 5) *Korean Journal of Metals and Materials* 56 (8) 2018: pp. 611 – 619. https://doi.org/10.3365/KJMM.2018.56.8.611

35. **Song, M.Y., Choi, E., Kwak, Y.J.** Raising the Dehydrogenation Rate of a Mg-CMC (Carboxymethylcellulose, Sodium Salt) Composite by Alloying Ni via Hydride-Forming Milling *Korean Journal of Metals and Materials* 56 (8) 2018: pp. 620 – 627. https://doi.org/10.3365/KJMM.2018.56.8.620

36. **Choi, E., Kwak, Y.J., Song, M.Y.** Development of an Mg-Based Alloy with a Hydrogen-Storage Capacity over 6 wt% by Adding Graphene *Metals and Materials International* 24 (6) 2018: pp. 1403 – 1411. https://doi.org/10.1007/s12540-018-0151-2

37. **Park, H.R., Kwak, Y.J., Song, M.Y.** Role of the added Ni in Hydrogen-Storage Reactions of MgH_2-$Zn(BH_4)_2$-Tm (Ni, Ti, or Fe) Alloys *Material Science* 24(4) 2018: pp. 376-381. http://dx.doi.org/10.5755/j01.ms.24.4.19051

38. **Song, M.Y., Kwak, Y.J.** Hydrogen Storage Properties of Mg Alloy Prepared by Incorporating Polyvinylidene fluoride via Reactive Milling *Korean Journal of Metals and Materials* 56(12) 2018: pp. 878-884. https://doi.org/10.3365/KJMM.2018.56.12.878

39. **Song, M.Y., Kwak, Y.J., Lee, S.H., Park, H.R.** Development of Mg-14Ni-6TaF_5 Hydrogen Absorption-Desorption Material via Reactive Mechanical Grinding *Materials Science (Medžiagotyra)* 20 (4) 2014: pp. 440 – 445.

https://doi.org/10.5755/j01.ms.20.4.6457

40. **Song, M.Y., Kwon, S.N., Park, H.R.** Addition of Oxides Fe_2O_3 and/or MnO to Improve Hydrogen Storage Properties of Magnesium by Reaction-Involved Milling *Journal of Ceramic Processing Research* 17 (8) 2016: pp. 851 – 857.

41. **Park, H.R., Lee, S.H., Song, M.Y.** Comparison of the Hydrogenation and Dehydrogenation Properties of Oxide and Halide-Added Mg Composites Prepared by Reactive Mechanical Grinding and Characterization of an Mg-$TiCl_3$ Composite *Journal of Ceramic Processing Research* 17 (12) 2016: pp. 1292 – 1298.

42. **Kwak, Y.J., Park, H.R., Song, M.Y.** Analysis of the Metal hydride Decomposition Temperatures of MgH_2 – $Zn(BH_4)_2$ – NaCl – Tm (Tm = Ni or Ti) Using a Sievert's Type Volumetric Apparatus *Materials Science (Medžiagotyra)* 23 (1) 2017: pp. 21 – 26. https://dx.doi.org/10.5755/j01.ms.23.1.14270